Therapeutic Interventions to Reduce Radiation Induced Dermal Injury in a Murine Model of Tissue Expander Based Breast Reconstruction

Alexandra O. Luby, MS,[a] Alicia E. Snider, MD,[b] Gurjit S. Mandair, PhD,[c] Kevin M. Urlaub, BS,[a] Jeremy V. Lynn, BS,[a] Noah S. Nelson, MPH,[a] Alexis Donneys, MD,[a] Russell E. Ettinger, MD,[d] Geoffrey C. Gurtner, MD,[e] David Kohn, PhD,[c] and Steven R. Buchman, MD[a]

Background: Radiation therapy (XRT) induced dermal injury disrupts type I collagen architecture. This impairs cutaneous viscoelasticity, which may contribute to the high rate of complications in expander-based breast reconstruction with adjuvant XRT. The objective of this study was to further elucidate the mechanism of radiation-induced dermal injury and to determine if amifostine (AMF) or deferoxamine (DFO) mitigates type I collagen injury in an irradiated murine model of expander-based breast reconstruction.

Methods: Female Lewis rats (n = 20) were grouped: expander (control), expander-XRT (XRT), expander-XRT-AMF (AMF), and expander-XRT-DFO (DFO). Expanders were surgically placed. All XRT groups received 28 Gy of XRT. The AMF group received AMF 30 minutes before XRT, and the DFO group used a patch for delivery 5 days post-XRT. After a 20-day recovery period, skin was harvested. Atomic force microscopy and Raman spectroscopy were performed to evaluate type I collagen sheet organization and tissue compositional properties, respectively.

Results: Type I collagen fibril disorganization was significantly increased in the XRT group compared with the control (83.8% vs 22.4%; $P = 0.001$). Collagen/matrix ratios were greatly reduced in the XRT group compared with the control group (0.49 ± 0.09 vs 0.66 ± 0.09; $P = 0.017$). Prophylactic AMF demonstrated a marked reduction in type I collagen fibril disorganization on atomic force microscopy (15.9% vs 83.8%; $P = 0.001$). In fact, AMF normalized type I collagen organization in irradiated tissues to the level of the nonirradiated control ($P = 0.122$). Based on Raman spectroscopy, both AMF and DFO demonstrated significant differential protective effects on expanded-irradiated tissues. Collagen/matrix ratios were significantly preserved in the AMF group compared with the XRT group (0.49 ± 0.09 vs 0.69 ± 0.10; $P = 0.010$). β-Sheet/α-helix ratios were significantly increased in the DFO group compared with the XRT group (1.76 ± 0.03 vs 1.86 ± 0.06; $P = 0.038$).

Conclusions: Amifostine resulted in a significant improvement in type I collagen fibril organization and collagen synthesis, whereas DFO mitigated abnormal changes in collagen secondary structure in an irradiated murine model of expander-based breast reconstruction. These therapeutics offer the ability to retain the native microarchitecture of type I collagen after radiation. Amifostine and DFO may offer clinical utility to reduce radiation induced dermal injury, potentially decreasing the high complication rate of expander-based breast reconstruction with adjuvant XRT and improving surgical outcomes.

Key Words: postmastectomy radiation, radiation injury, irradiated breast reconstruction, breast reconstruction after radiotherapy, expander-based breast reconstruction, amifostine, deferoxamine, type I collagen, atomic force microscopy, Raman spectroscopy

(*Ann Plast Surg* 2020;85: 546–552)

Breast cancer is the most common malignancy among women in the United States. In recent years, there have been expansions in the indications for adjuvant radiation therapy (XRT).[1–3] Although radiotherapy is a vital component of breast cancer treatment, shown to reduce disease recurrence and increase survivorship, it poses significant challenges to breast reconstruction.[4,5] Implant-based reconstruction is especially difficult to achieve for this subset of patients, because this approach is plagued by wound breakdown and implant exposure as well as the inability to attain appropriate volume because of fibrosis and contracture of the dermis in the setting of postmastectomy radiation therapy (PMRT).[4,5] In fact, radiation was found to be one of the greatest risk factors for major complications in implant-based reconstruction.[3] As such, recent studies have advocated for the use of autologous reconstruction as the most conservative approach after PMRT[1,2,5]; however, not all patients are candidates or desire autologous reconstruction. Despite the high complication rate, however, expander- and implant-based reconstruction still continue to be used in the setting of PMRT. Therefore, reducing complications in expander- and implant-based breast reconstruction after PMRT is of great clinical interest.

Despite technologic advancements, radiotherapy induces collateral damage to the surrounding skin, soft tissue, and vasculature. This often manifests as chronic dermatitis and hyperpigmentation but more significantly can result in reduced skin vascularity, impaired wound healing, and fibrosis, which significantly impacts the outcomes of implant-based breast reconstruction after PMRT.[6,7] At the cellular level, radiation causes direct DNA damage and the generation of free radicals, which induces oxidative stress and ultimately incites changes within the microarchitecture of the skin.[8] Radiation-induced dermal damage can disrupt normal homeostasis of fibrillar type I collagen, the major

Received September 4, 2019, and accepted for publication, after revision December 5, 2019.

From the [a]Section of Plastic Surgery Craniofacial Research Laboratory, Department of Surgery, University of Michigan Health System, Ann Arbor, MI; [b]Department of Surgery, School of Medicine, University of South Carolina, Columbia, SC; [c]Department of Chemistry, University of Michigan Medical School, Ann Arbor, MI; [d]Division of Plastic Surgery, Department of Surgery, University of Washington, Seattle, WA; and [e]Department of Surgery, Stanford University, Stanford, CA.

A.O.L. and A.E.S. have equal contribution and share first authorship.

Conflicts of interest and sources of funding: The authors have no conflicts of interest that are associated with this publication. This work was supported by National Institutes of Health grant NIH-R01 CA 125187-06 awarded to S.R.B. This work was also supported by an NIH T-32 Training Grant (GM 8616-17) awarded to A.E.S. In addition, this work was supported by a PSF Pilot Grant from the Plastic Surgery Foundation (N021718). This work also received support from the NIH-NIAMS P30 Grant awarded to the University of Michigan (NIH/NIAMS 069620). The following patent is assigned to G.C.G. and Stanford University: Topical and Transdermal Delivery of HIF-1 Modulators to Prevent and Treat Chronic Wounds (20100092546).

Atomic force microscopy results were presented on September 28, 2018 at ASPS 87th Annual Meeting in Chicago, IL. Raman spectroscopy results were presented on September 22, 2019 at ASPS 88th Annual Meeting in San Diego, CA.

Reprints: Steven R. Buchman, MD, Section of Plastic Surgery Craniofacial Research Laboratory, Department of Surgery, University of Michigan Health System, C.S. Mott Children's Hospital, 1540 E Hospital Dr, SPC-4219, Ann Arbor, MI 48109. E-mail: sbuchman@med.umich.edu (S.R.B.).

Supplemental digital content is available for this article. Direct URL citations appear in the printed text and are provided in the HTML and PDF versions of this article on the journal's Web site (www.annalsplasticsurgery.com).

ISSN: 0148-7043/20/8505–0546
DOI: 10.1097/SAP.0000000000002264

structural protein in the skin, which is critical for maintaining skin architecture and providing the substrate for adequate wound healing.[8] When collagen organization and synthesis are undermined, the viscoelastic properties of the skin are compromised, which poses obstacles to tissue expansion.[9,10] As such, XRT-induced dermal damage can ultimately limit patient candidacy for implant- and expander-based breast reconstruction, as significant skin fibrosis restricts the extent of achievable expansion.[11] Preserving dermal integrity and type I collagen organization represents a potential method to facilitate improved breast reconstructive outcomes after radiotherapy, especially in expander- and implant-based approaches.

Currently, there are no therapeutics available to reduce collateral damage of skin and soft tissue after XRT in breast cancer patients. Given the increasing indications for adjuvant radiotherapy in breast cancer treatment, methods to minimize collateral tissue damages due to XRT would offer tremendous clinical utility. Amifostine (AMF) is one of only a few Food and Drug Administration–approved radioprotective agents, shown to mitigate radiation induced complications in patients receiving radiotherapy for head and neck cancer treatment. Previous investigations in our laboratory have identified AMF as a potential therapeutic solution to radiation injury in breast cancer patients, because it demonstrated significant remediation of radiation-induced cutaneous and vascular injury in a murine model of expander-based breast reconstruction.[12,13] Deferoxamine (DFO) is a Food and Drug Administration–approved iron chelator used to treat iron overload for patients with hemochromatosis. Previous work in our laboratory has demonstrated that DFO mitigates radiation-induced injury to bone, as well as to the skin and soft tissues.[8,14] In fact, one recent study in our laboratory investigated the use of topical DFO in an irradiated, expander-based breast reconstruction model, in which DFO treatment demonstrated significant remediation of cutaneous ulceration and dermal type I collagen fibril disarray. Therefore, the current study served to further investigate the mechanism of radiation-induced dermal injury and to determine if AMF and/or DFO assuages type I collagen injury at the level of the collagen fibril and collagen sheet. To study this, we used AMF as a prophylactic radioprotective therapeutic and DFO as a post-XRT in a murine model of irradiated expander-based breast reconstruction. Our specific metrics of interest were atomic force microscopy (AFM) to evaluate surface properties of type I collagen and Raman spectroscopy to evaluate the chemical composition of the tissue.

MATERIALS AND METHODS

Study Design

All animal studies were approved by the University of Michigan's Institutional Animal Care and Use Committee before implementation. All animal experimentation was performed according to the guidelines published in the *Guide for the Care and Use of Laboratory Animals, Eighth Edition*. Adult female Sprague-Dawley rats (n = 20) weighing approximately 350 g were obtained and acclimated for 7 days. Animals were then randomly assigned to experimental groups: (1) expander placement (control); (2) expander placement–XRT (XRT); (3) expander-XRT-AMF (AMF); and (4) expander-XRT-DFO (DFO) (Fig. 1).

Surgical Procedure

Our surgical procedure has been previously described and published.[12,13] In summary, a 3-cm longitudinal incision was made 1 cm to the right of dorsal midline. A submusculocutaneous pocket was made using blunt dissection to achieve an appropriate size to accommodate the tissue expander. A sterile, silicon-based, smooth-textured mini-expander (Allergan, Inc, Santa Barbara, CA) measuring 3 cm in diameter was placed in the tissue pocket. The tissue expander port (2 cm distal; diameter, 1.5 cm; height, 0.6 cm) was positioned caudally and secured with a single 4-0 monocryl suture. The muscle and skin were reapproximated over the expander using interrupted 4-0 Vicryl sutures. Postoperative recovery was ensured by monitoring the animals during their recovery from anesthesia and using warming and oxygen as needed.

Expansion and Recovery

Animals received daily operative site monitoring for 14 days postoperatively. Analgesia with buprenorphine was continued every 12 hours through postoperative day (POD) 4, and daily weights were obtained to monitor nutritional status until POD 10. Tissue expansion took place under isoflurane drop anesthesia on PODs 15, 18, and 21 (Fig. 2). During expansion, 5 mL of 0.9% normal saline was injected during each session to achieve a total fill volume of 15 mL. This total fill volume was determined based on the tension and compliance of the expanded tissue overlying the implant as previously described.[12,13]

Radiation Procedure

All radiation procedures were conducted in the Irradiation Core at the University of Michigan. After consultation with Radiation Oncology at the University of Michigan, a total radiotherapy dose of 28 Gy was delivered as 5.6 Gy per day over 5 days beginning on POD 22. Clinically, adjuvant XRT is administered after tissue expansion. Therefore, we chose to this time point to parallel this process. After transient induction of anesthesia with an oxygen/isoflurane mixture, select rats were radiated using a Philips RT250 orthovoltage unit (250 kV, 15 mA) (Kimtron, Inc, Oxford, CT). A lead shield with a 3.5-cm diameter circular aperture was used to ensure localized delivery of radiation to our selected region of interest corresponding with the area of expanded tissue.

AMF Treatment

Animals in the AMF group received a radioprotective dose of 100 mg/kg of AMF 20 minutes before radiotherapy. This dosing is consistent with previous work in our laboratory, demonstrating this to be an effective radioprotective dose of AMF.

DFO Treatment

In collaboration with the Bioengineering and Materials Science Laboratory at Stanford University, we developed a topical formulation of DFO to allow for transcutaneous delivery. These DFO patches were formulated as previously described.[8] Deferoxamine patches were dosed at 2 mg (1 mg/cm^3) to deliver effective radiation remediating doses, as demonstrated in our previous studies. To enable transcutaneous drug delivery, hair overlying the tissue expander was removed. Deferoxamine

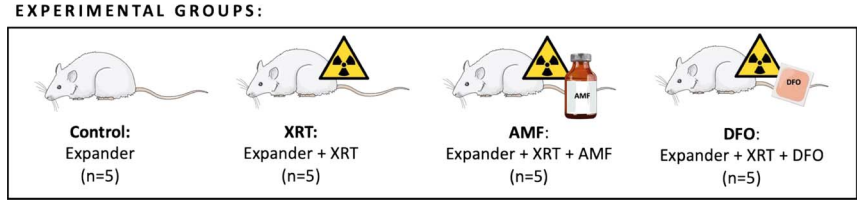

FIGURE 1. Summary of experimental groups. full color online

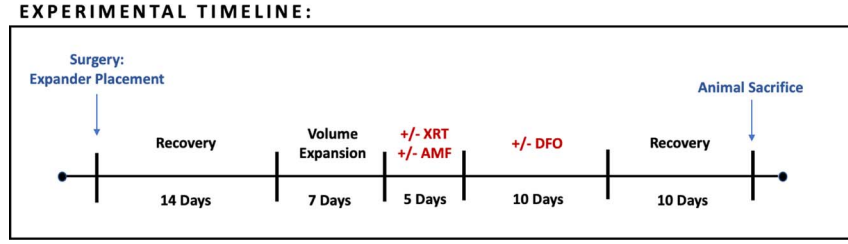

FIGURE 2. Summary of experimental timeline. full color online

patches were secured to the expanded tissues using Transpore tape. Deferoxamine treatment was started on the day after the final day of XRT and continued for 10 days. Elizabethan collars were used to reduce grooming of the expander and retain the DFO patch treatment on the area of the expanded tissue. Notably, all animals in this study received Elizabethan collars to reduce potential confounding between groups.

AFM Analysis of Collagen Organization

Atomic force microscopy was only performed for control, XRT, and AMF groups (n = 5 per group), because DFO was investigated in a previous study.[8] Twenty days after radiation, animals underwent euthanasia via systemic paraformaldehyde perfusion.[12,13] Skin tissue sections of 25-μm thickness were prepared parallel to the dermal horizontal plane. Atomic force microscopy was used to determine the micrometer-scale architecture,[15] analyzing organization of the collagen fibril sheet, as previously described.[8] To briefly summarize, AFM imaging was ascertained in contact mode using Anasys Instruments contact mode nanoIR2 probes (silicon cantilever with gold coating; nominal radius, 25 nm; resonance frequency, 13 ± 4 kHz; spring constant, 0.07–0.4 N/m; length, 225 nm). Images measuring 10 μm × 10 μm with a line scan rate of 1.0 Hz and 512 pixels per line (~19.5 nm/pixel) were obtained and used for evaluation of type I collagen fibril sheet organization. Collagen sheets with 2 or more collagen fibrils organized in parallel were defined a region of type I collagen organization. Microarchitecture analysis was performed by 2 independent, blinded reviewers using ImageJ analysis to quantify the percentage of dermal collagen fibril organization per unit area within the AFM images. The average value of the 2 reviewers was used for statistical analysis.

Raman Spectroscopy

Raman spectroscopy was performed for all 4 rodent groups in this study: control, XRT, AMF, and DFO. Skin tissue sections embedded in O.C.T. compound (Tissue-Tek; Sakura Finetek USA, Inc, Torrance, CA) were thawed and imaged using an SMZ800 stereomicroscope (Nikon Instruments, Inc). The images were used to identify expanded tissue regions for compositional and structural analysis by Raman spectroscopy. The O.C.T. compound surrounding the tissue sections was removed by dissolution in phosphate-buffered saline (PBS) solution before analysis. Briefly, the tissue section was transferred into a wide Petri dish containing PBS solution and agitated on a Titer plate shaker (Lab-line Instruments, Melrose Park, IL). The agitated solution was periodically replaced with fresh PBS solution over a 20-minute period. The cleaned tissue section was then analyzed by Raman spectroscopy under hydrated conditions.

Tissue compositional analysis was carried out using the RamanRxn1 spectrometer (Kaiser Optical Systems, Inc, Ann Arbor, MI) as described in detail elsewhere.[15] The spectrometer was equipped with a near-infrared laser (Invictus 785-nm laser) and a stainless-steel fiberoptic probe (0.27 numerical objective, laser spot size of ~100 μm, and power output of ~87 mW). Tissue spectra were acquired from the following 4 rodent groups (n = 7 per group): control, XRT, AMF, and DFO. For each tissue section, 8 to 12 spectra were acquired using 6 × 10 second acquisitions (Andor Solis Software; Andor Technologies, Belfast, Northern Ireland, United Kingdom).

Spectroscopic Analysis of Tissue Composition

Spectra were processed and calibrated in MATLAB Software (The MathWorks Inc, Natick, MA) and then imported into GRAMS/AI Software (Thermo Fisher Scientific, Inc, Waltham, MA) for baseline correction and normalization.[16] For curve-fitting analyses, second derivative and constrained Gaussian deconvolution functions were applied to the following spectral regions: 800 to 1020 cm^{-1} (806, 814, 820, 839, 854, 864, 876, 884, 890, 896, 902, 914, 921, 938, 950, 959, 968, 978, 1003, and 1014 cm^{-1}) and 1536 to 1721 cm^{-1} (amide I region, 1541, 1548, 1555, 1564, 1574, 1585, 1594, 1603, 1616, 1632, 1644, 1656, 1671, 1687, 1700, and 1711 cm^{-1}). Tentative band assignments were made for the following select tissue components: tyrosine (Tyr) δ(C-CH) aliphatic band at approximately 832 cm^{-1} (buried Tyr conformation), Tyr δ(C-CH) aromatic band at approximately 850 cm^{-1} (exposed Tyr conformation, with ring proline collagen ν(C-C) contribution), ring hydroxyproline collagen ν(C-C) band at approximately 876 cm^{-1}, and amide I ν(C=O) matrix protein bands at approximately 1656 cm^{-1} (α-helix conformation) and approximately 1671 cm^{-1} (β-sheet conformation).[17,18] These bands were then used in subsequent Raman ratiometric analyses because of their limited spectral interference from tissue lipid components and the sapphire window of the fiberoptic probe. Select height ratios were then used to calculate the following 3 tissue compositional or structural properties: collagen/matrix (854 + 876)/1656 cm^{-1}), Tyr buried/exposed (832/854 cm^{-1}), and collagen β-sheet/α-helix (1671/1656 cm^{-1}) ratios. A low Tyr buried/exposed ratio indicates more exposed protein Tyr side chains with a higher ability to bind to water molecules, whereas a larger ratio indicates more buried protein Tyr side chains with a limited ability to bind to water molecules[18] and high collagen/matrix ratios indicate increased collagen content or turnover.[16,19,20] Collagen β-sheet/α-helix ratio provides information on collagen secondary structure, with high ratio values reflecting a higher relative proportion of β-sheet conformation to α-helical conformation.[18,21]

Statistical Analysis

All between-group skin ulceration, collagen disorganization, or tissue composition statistical analyses were performed in SPSS Software for Windows (IBM SPSS Statistics 26, IBM Corp, NY). Post hoc Tukey (paramagnetic) or Games-Howell (nonparamagnetic) significance difference tests ($P < 0.05$) were run depending on the homogeneity of variances as per the Levene test ($P < 0.05$).[7] Power analyses were also performed in nQuery Advisor Software (Statistical Solutions, Saugus, MA) with assistance from the University of Michigan Center for Statistical Consultation and Research.[8,22] Only between-group comparisons that were sufficiently powered to claim statistical significance at 80% power (2-sided, $\alpha = 0.05$) were accepted in this study. Spearman's correlation coefficient (ρ, "rho") and Kendall's correlation coefficient (τ, "tau") between pooled covariate collagen disorganization and tissue compositional variables were calculated in SPSS Software. Statistical significance was accepted at the $P < 0.05$ level.

RESULTS

AFM Analysis of Type I Collagen Organization

Atomic force microscopy images of dermal type I collagen are summarized in Figure 3. On ImageJ analysis of the AFM imaging, the XRT group exhibited approximately 4 times the degree of type I collagen disorganization compared with the control (83.8% vs 22.4%; $P = 0.001$) (Fig. 4). Treatment with AMF before radiotherapy resulted in greater than a 4-fold reduction in collagen disorganization. The AMF group exhibited preserved collagen sheet organization with only 15.9% disorganization compared with the XRT group ($P = 0.001$). In fact, AMF preserved dermal collagen organization to the level of the nonirradiated controls receiving tissue expansion alone, indicating that AMF mitigates radiation-induced fibril disarray. As such, no statistical differences were identified between control and AMF groups (22.4% vs 15.9%; $P = 0.122$) because both demonstrated similar parallel, organized collagen sheets.

Raman Spectroscopy

Tissue composition and structure between control, XRT, AMF, and DFO groups were examined by Raman spectroscopy using the Games-Howell statistical significance test ($P < 0.05$). Collagen/matrix ratios were significantly reduced in the XRT group compared with the control group (0.49 ± 0.09 vs 0.66 ± 0.09; $P = 0.017$) but was significantly preserved in the AMF group (0.49 ± 0.09 vs 0.69 ± 0.10; $P = 0.010$) (Fig. 5). In contrast, no significant differences in collagen/matrix ratios were found between the XRT and DFO groups (0.49 ± 0.09 vs 0.63 ± 0.18; $P = 0.347$) or the control and AMF or DFO groups ($P = 0.995$ and $P = 0.976$, respectively). To evaluate the impact of radiotherapy on skin barrier function, tyrosine buried/exposed ratios were calculated. Tyrosine (Tyr) buried/exposed ratios were nonsignificantly increased in the XRT group compared with the control group (0.38 ± 0.16 vs 0.20 ± 0.05; $P = 0.082$) but marginally reduced compared with the AMF (0.38 ± 0.16 vs 0.17 ± 0.10; $P = 0.059$) and DFO (0.38 ± 0.16 vs 0.23 ± 0.13; $P = 0.057$) groups (Fig. 6). No significant differences in Tyr buried/exposed ratios were found between the control and AMF or DFO groups ($P = 0.935$ and $P = 0.938$, respectively). When secondary structure was examined (Fig. 7), collagen β-sheet/α-helix ratios were nonsignificantly reduced in the XRT group compared with the control (1.76 ± 0.03 vs 1.80 ± 0.04; $P = 0.365$) and AMF (1.76 ± 0.03 vs 1.81 ± 0.05; $P = 0.285$) groups but was significantly increased in the DFO group (1.76 ± 0.03 vs 1.86 ± 0.06; $P = 0.038$). No significant differences in collagen β-sheet/α-helix ratios were identified between the control and AMF or DFO groups ($P = 0.972$ and $P = 0.242$, respectively).

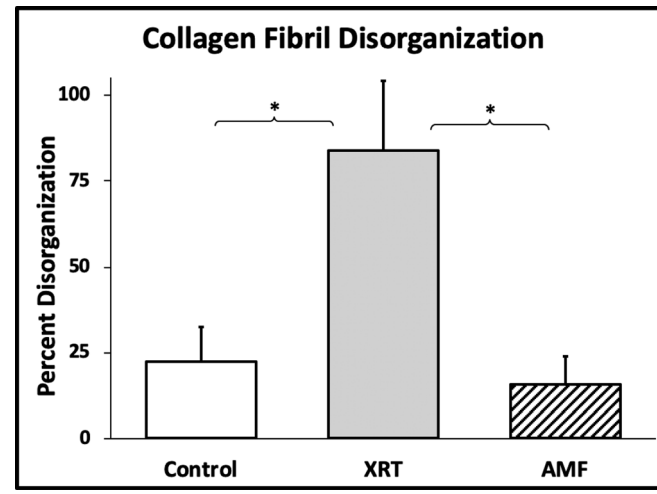

FIGURE 4. Type I collagen fibril disorganization. Fibril disorganization increased significantly in XRT group compared with control. Radiation therapy–induced collagen disorganization was mitigated by AMF. *$P < 0.05$.

Linear relationships between AFM-derived percent collagen type I disorganization and Raman spectroscopic measures of tissue composition and structure were examined after pooling the data from all 4 rodent groups (Supplementary Fig. 1, http://links.lww.com/sap/A459). As shown by the Spearman ρ and Kendall τ values in Table 1, significant positive linear correlations were found between percent collagen disorganization and collagen β-sheet/α-helix ratios ($\rho = 0.545$ and $\tau = 0.422$; $P = 0.003$ and $P = 0.002$, respectively) and Tyr buried/exposed ratios ($\rho = 0.409$ and $\tau = 0.308$; $P = 0.034$ and $P = 0.024$, respectively). In contrast, a negative nonsignificant correlation was found between collagen disorganization and collagen/matrix ratios ($\rho = -0.205$ and $\tau = -0.145$; $P = 0.305$ and $P = 0.288$, respectively).

DISCUSSION

This study further elucidates the mechanism of radiation-induced dermal type I collagen injury. Radiotherapy significantly increased type I collagen fibril disorganization on AFM. Differences in tissue composition and collagen secondary structure between the irradiated and nonirradiated control groups were also identified using Raman spectroscopy. More specifically, collagen/matrix ratios, a surrogate measure of tissue collagen content, were significantly decreased in the irradiated group compared with the nonirradiated control. In addition,

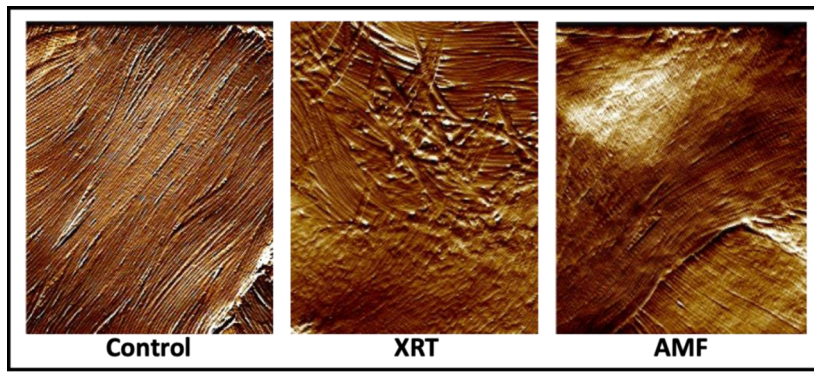

FIGURE 3. Atomic force microscopy images. The XRT group demonstrated significantly greater fibril disorganization than the control. Amifostine preserved collagen organization to control levels. full color online

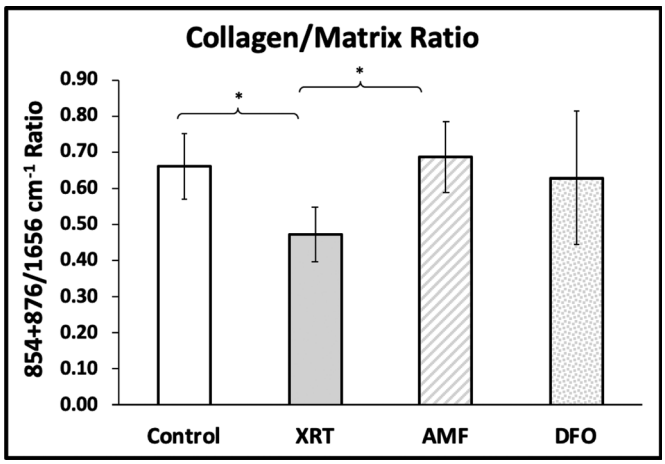

FIGURE 5. Collagen/matrix ratio. The XRT group exhibits a significantly lower collagen/matrix ratio compared with the control group. This ratio is restored in the AMF group but only partially in the DFO group. *$P < 0.05$.

collagen β-sheet/α-helix ratios, a representative measure of collagen secondary structure, were reduced in the irradiated group compared with the control. Moreover, linear regression analyses revealed significant positive correlations between tissue-level collagen secondary structure by Raman spectroscopy and collagen ultrastructural fibril organization by AFM. To our knowledge, this is the first study in a breast reconstruction model where AFM and Raman spectroscopic measurements were regressed against each other. This positive correlation suggests that dermal collagen fibril organization is related to the maintenance of tissue collagen secondary structure.

In addition, when intensity ratios between Tyr-specific Raman bands were examined, irradiated tissues exhibited a trend of increased Tyr buried/exposed ratios compared with nonirradiated tissues. We hypothesize that the increased buried Tyr conformations in irradiated tissues resulted from the limited ability of its hydroxyl side groups to bind to local water molecules.[17,22] The latter finding may be related to the well-known phenomena of transepidermal water loss after radiotherapy[23–26] and suggests that Tyr buried/exposed ratios could be used as a surrogate marker for evaluating changes in skin barrier function. Furthermore, given that collagen secondary structure is sensitive

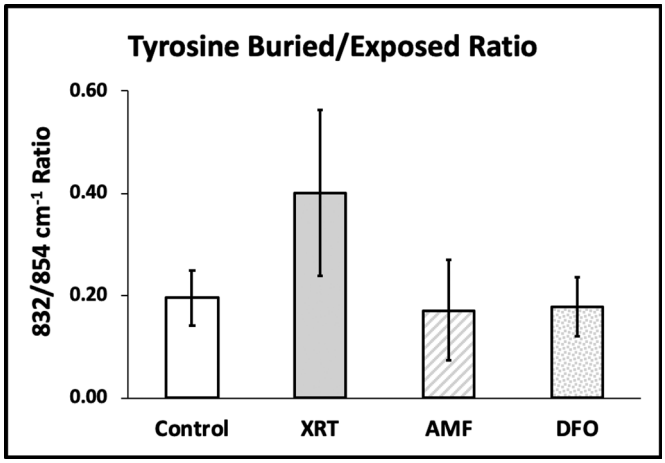

FIGURE 6. Tyrosine buried/exposed ratio. The AMF and DFO groups exhibit a nonsignificant normalization of the Tyr buried/exposed ratio compared with the XRT group.

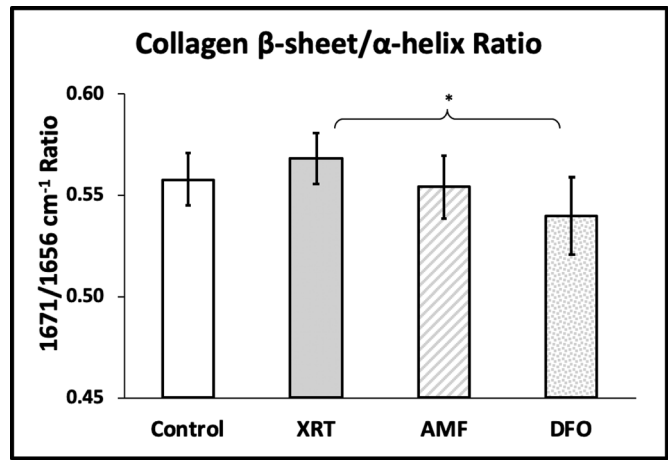

FIGURE 7. Collagen β-sheet/α-helix ratio. The DFO group exhibits a significantly lower β-sheet conformation compared with the XRT group. *$P < 0.05$.

to changes in water content,[27] we speculate that the increased type I collagen fibril disorganization and reduced collagen β-sheet content detected after radiation in this study may be indirectly related to changes in tissue hydration.

In addition to further illuminate the mechanism of radiation-induced collagen injury, this study investigated the potential utility of 2 therapeutics, DFO and AMF, to reduce dermal type I collagen injury in irradiated, expanded tissues. In this study, DFO was administered as a postradiation topical patch, whereas AMF was administered subcutaneously as a prophylactic treatment. In a previous study in our laboratory, the topical DFO patch was shown to mitigate type I collagen fibril disorganization,[8] which supports our hypothesis that skin barrier function is linked to fibril organization. In the current study, DFO remediated radiation-induced losses in α-helical collagen content, as resulting collagen β-sheet/α-helix ratios were significantly reduced compared with the irradiated control. These findings suggest that perhaps the key to mitigating alterations in type I collagen secondary structure and fibril organization is to prevent fluctuations in tissue hydration by reducing transepidermal water losses after radiotherapy. Furthermore, prophylactic radioprotection with AMF resulted in a significant preservation in collagen organization in irradiated tissues on AFM. In fact, AMF normalized collagen organization to the level of the nonirradiated controls by inhibiting derangements in collagen organization caused by radiotherapy. Amifostine pretreatment also prevented the abnormal decline in collagen/matrix ratio that is characteristic of irradiated tissues. In fact, this surrogate for collagen content was normalized in AMF tissues and preserved to the level of the nonirradiated control. Taken together, our findings demonstrate the proficiency of both DFO and AMF to mitigate distinct aspects of radiation-induced dermal type I collagen injury. These findings are meaningful, because developing methods to preserve type I collagen may allow for improved viscoelastic properties of the skin after radiotherapy, which has to potential to increase patient

TABLE 1. Correlations Between AFM and Raman Spectroscopic Findings

Raman Parameter	Spearman's ρ	P (ρ)	Kendall's τ	P (τ)
Collagen β-sheet/α-helix ratio	0.545	0.003	0.422	0.002
Tyr buried/exposed ratio	0.409	0.034	0.308	0.024
Collagen/matrix ratio	−0.205	0.305	−0.145	0.288

candidacy for expander- and implant-based breast reconstruction and improve outcomes after PMRT.

Whereas these results propose that AMF and DFO therapy can significantly reduce the pathologic effects of radiotherapy on dermal type I collagen as singular therapies, the findings of this study also suggest that AMF and DFO may be increasingly efficacious in combination. Whereas AMF reduces radiation injury to healthy tissue at the time of radiotherapy, DFO works to salvage the effects of radiation in the days after radiotherapy. Both DFO and AMF were shown to significantly reduce type I collagen disorganization after XRT.[8] Deferoxamine, however, reduced alterations in collagen secondary structure, whereas AMF mitigated abnormal changes in collagen content and synthesis in irradiated tissues. Because DFO and AMF seem to produce differential effects on irradiated, expanded tissues, there could great utility in applying these therapeutics in combination. Administering AMF before radiotherapy and DFO afterwards may produce a summative or synergistic effect to improve skin and soft tissue quality after radiotherapy. Although further investigation is required to validate this hypothesis, the results in this study are promising and build upon our previous findings in this irradiated model of breast reconstruction.

Currently, there are no therapeutics to prevent collateral damage to the surrounding skin, soft tissue, and vasculature in breast cancer patients receiving adjuvant XRT. Therefore, high complication rates associated with breast reconstruction after radiotherapy remain a major challenge. Radiation induces significant short- and long-term deleterious effects on the skin, soft tissue, and surrounding vasculature. Complex cellular alterations and inflammatory cascades ensue in the aftermath of radiotherapy, contributing to the pathogenesis of poor wound healing, fibrosis, and reduced tissue perfusion after radiotherapy. Fibrosis, in particular, results from collagen resorption, aberrant deposition, and disorganization after radiation,[28] which significantly impairs the viscoelastic properties of skin required for successful tissue expansion. Therefore, radiation-induced skin fibrosis poses significant challenges to implant- and expander-based breast reconstruction and, in severe cases, may be necessarily eschewed entirely in irradiated patients. Patients undergoing postradiotherapy breast reconstruction have higher complication rates overall and often experience delayed or less satisfactory aesthetic results because of wound breakdown and implant exposure as well as the inability to attain appropriate volume because of fibrosis and contracture of the dermis in the setting of PMRT. In this study, we have identified 2 therapeutics, DFO and AMF, which significantly reduce the pathologic effects of radiotherapy on dermal type I collagen. This is a propitious finding that could significantly improve the current standard of care for implant based breast reconstruction requiring radiotherapy.

Although the results of this study are promising, there are a few limitations we must address. Raman spectroscopic measures of collagen/matrix ratios were not calibrated to provide absolute measures of collagen content for a given quantity of skin tissue; however, the measurement was based on similar spectroscopic ratios that had been used to assess relative changes in soft and hard tissue specimens.[16,19,20,29] Given the importance of tissue hydration to skin barrier function, further studies evaluating additional noninvasive techniques to quantify tissue water content would be beneficial to determine how the results compare with corresponding Raman spectroscopic techniques.[23,25] In addition, one limitation of this study is the exclusion of a sham patch control group. This additional control would provide insight whether the patch alone may be contributing to the hydration barrier effect demonstrated by the DFO patch. The sham patch control will be assessed in future investigations. In this study, AMF and DFO were highly effective at mitigating radiation-induced dermal type I collagen injury. One important future study, however, is investigating the oncologic safety of using AMF and DFO in breast cancer patients, who could have potential disease recurrence. Although reducing the burden of the deleterious effects of radiation has the potential to significantly improve quality of life for breast cancer survivors, we need to determine if these therapies are oncologically safe for use in these patients. These studies are currently underway in our laboratory. In addition, although the results of this study are promising, further investigation is warranted to determine if there is a potential synergistic effect of using AMF and DFO in combination. We posit that AMF and DFO may be highly efficacious in combination, because they seem to reduce radiation injury through different mechanisms and at different intervention time points based on the results of this study.

CONCLUSIONS

In this study, we have identified DFO and AMF as potential therapeutics to reduce radiation injury in breast cancer patients undergoing expander-based breast reconstruction. Our findings suggest that AMF and DFO both significantly reduce dermal type I collagen disorganization associated with radiotherapy; however, each therapy seems to act through different mechanisms. Topical DFO reduced abnormal alterations in collagen secondary structure. Prophylactic AMF preserved collagen content and synthesis in irradiated tissues, preventing aberrant changes in collagen turnover associated with radiotherapy. The results of this study identify DFO and AMF as potential therapeutics to mitigate radiation-induced dermal type I collagen injury in irradiated breast reconstruction. Given that DFO and AMF work through different mechanisms to produce distinct radioprotective and radiation salvage effects, we predict that AMF and DFO may be increasingly efficacious in combination, which will be the focus of some of our future work. The utilization of AMF and DFO as novel therapeutics to reduce radiation induced dermal injury may have great clinical utility in improving surgical outcomes and increasing patient candidacy for the operation by potentially decreasing the high complication rate of expander-based breast reconstruction associated with adjuvant XRT.

REFERENCES

1. Ho A-Y, Hu Z-I, Mehrara B-J, et al. Radiotherapy in the setting of breast reconstruction: types, techniques, and timing. *Lancet Oncol*. 2017;18:e742–e753.
2. Billig J, Jagsi R, Qi J, et al. Should immediate autologous breast reconstruction be considered in women who require post-mastectomy radiation therapy? A prospective analysis of outcomes. *Plast Reconstr Surg*. 2017;139:1279–1288.
3. Kronowitz S-J, Robb G-L. Radiation therapy and breast reconstruction: a critical review of the literature. *Plast Reconstr Surg*. 2009;124:395–408.
4. Jagsi R, Momoh A-O, Qi J, et al. Impact of radiotherapy on complications and patient-reported outcomes after breast reconstruction. *J Natl Cancer Inst*. 2017; 110:157–165.
5. Ricci J-A, Epstein S, Momoh A-O, et al. A meta-analysis of implant-based breast reconstruction and timing of adjuvant radiation therapy. *J Surg Res*. 2017;218: 108–116.
6. Perez-Aso M, Mediero A, Low Y-C, et al. Adenosine A2A receptor plays an important role in radiation-induced dermal injury. *FASEB J*. 2015;30:457–465.
7. Lee J-W, Zoumalan R-A, Valenzuela C-D, et al. Regulators and mediators of radiation-induced fibrosis: gene expression profiles and a rationale for Smad3 inhibition. *Otolaryngol Head Neck Surg*. 2010;143:525–530.
8. Snider A-E, Lynn J-V, Urlaub K-M, et al. Topical deferoxamine alleviates skin injury and normalizes atomic force microscopy patterns following radiation in a murine breast reconstruction model. *Ann Plast Surg*. 2018;81:604–608.
9. Qin Z, Robichaud P, He T, et al. Oxidant exposure induces cysteine-rich protein 61 (CCN1) via c-Jun/AP-1 to reduce collagen expression in human dermal fibroblasts. *PLoS One*. 2014;9:e115402.
10. Langton A-K, Graham H-K, McConnell J-C, et al. Organization of the dermal matrix impacts the biomechanical properties of skin. *Br J Dermatol*. 2017;177: 818–827.
11. Rodriguez J-J, Kung T, Wang Y, et al. Changes in skin vascularity in a murine model for post-mastectomy radiation. *Ann Plast Surg*. 2016;76:494–498.
12. Felice P-A, Nelson N-S, Page E-E, et al. Amifostine reduces radiation-induced complications in a murine model of expander-based breast reconstruction. *Plast Reconstr Surg*. 2014;134:551e–560e.
13. Polyatskaya Y, Nelson N-S, Rodriguez J-J, et al. Prophylactic amifostine prevents a pathologic vascular response in a murine model of expander-based breast reconstruction. *J Plast Reconstr Aesthet Surg*. 2016;69:234–240.

14. Donneys A, Nelson N-S, Perosky J-E, et al. Prevention of radiation-induced bone pathology through combined pharmacologic cytoprotection and angiogenic stimulation. *Bone*. 2016;84:245–252.
15. Cauble M-A, Rothman E, Welch K, et al. Alteration of type I collagen microstructure induced by estrogen depletion can be prevented with drug treatment. *Bonekey Rep*. 2015;4:697.
16. Bigelow E-M, Patton D-M, Ward F-S, et al. External bone size is a key determinant of strength-decline trajectories of aging male radii. *J Bone Miner Res*. 2019;34:825–837.
17. Leroy M, Labbe J-F, Ouellet M, et al. A comparative study between human skin substitutes and normal human skin using raman microspectroscopy. *Acta Biomater*. 2014;10:2703–2711.
18. Choe C, Schleusener J, Lademann J, et al. Keratin-water-nmf interaction as a three layer model in the human stratum corneum using in vivo confocal raman microscopy. *Sci Rep*. 2017;7:15900.
19. Lietman C-D, Lim J-Y, Grafe I, et al. Fkbp10 deletion in osteoblasts leads to qualitative defects in bone. *J Bone Miner Res*. 2017;32:1354–1367.
20. Bi X-H, Grafe I, Ding H, et al. Correlations between bone mechanical properties and bone composition parameters in mouse models of dominant and recessive osteogenesis imperfecta and the response to anti-TGF-β treatment. *J Bone Miner Res*. 2017;32:347–359.
21. Mandair G-S, Han A-L, Keller E-T, et al. Raman microscopy of bladder cancer cells expressing green fluorescent protein. *J Biomed Opt*. 2016;21:115001.
22. Donneys A, Ahsan S, Perosky J-E, et al. Deferoxamine restores callus size, mineralization, and mechanical strength in fracture healing after radiotherapy. *Plast Reconstr Surg*. 2013;131:711e–719e.
23. Schmuth M, Sztankay A, Weinlich G, et al. Permeability barrier function of skin exposed to ionizing radiation. *Arch Dermatol*. 2001;137:1019–1023.
24. Ryan J-L. Ionizing radiation: the good, the bad, and the ugly. *J Invest Dermatol*. 2012;132:985–993.
25. Robijns J, Censabella S, Claes S, et al. Biophysical skin measurements to evaluate the effectiveness of photobiomodulation therapy in the prevention of acute radiation dermatitis in breast cancer patients. *Support Care Cancer*. 2019;27:1245–1254.
26. Vyumvuhore R, Tfayli A, Duplan H, et al. Effects of atmospheric relative humidity on stratum corneum structure at the molecular level: ex vivo raman spectroscopy analysis. *Analyst*. 2013;138:4103–4111.
27. Nguyen T-T, Happillon T, Feru J, et al. Raman comparison of skin dermis of different ages: focus on spectral markers of collagen hydration. *J. Raman Spectroscopy*. 2013;44:1230–1237.
28. Jacobson L-K, Johnson M-B, Dedhia R-D, et al. Impaired wound healing after radiation therapy: a systematic review of pathogenesis and treatment. *JPRAS Open*. 2017;13:92–105.
29. Burke M-V, Atkins A, Akens M, et al. Osteolytic and mixed cancer metastasis modulates collagen and mineral parameters within rat vertebral bone matrix. *J Orthop Res*. 2016;34:2126–2136.